



Contents lists available at ScienceDirect

## European Journal of Medicinal Chemistry

journal homepage: <http://www.elsevier.com/locate/ejmech>

## Targeting transthyretin in Alzheimer's disease: Drug discovery of small-molecule chaperones as disease-modifying drug candidates for Alzheimer's disease



Ellen Y. Cotrina<sup>a</sup>, Luis Miguel Santos<sup>b, c</sup>, Josep Rivas<sup>d</sup>, Daniel Blasi<sup>d</sup>, José Pedro Leite<sup>b, c, e</sup>, Márcia A. Liz<sup>b, c</sup>, Maria Antònia Busquets<sup>f</sup>, Antoni Planas<sup>g</sup>, Rafel Prohens<sup>h</sup>, Ana Gimeno<sup>i</sup>, Jesús Jiménez-Barbero<sup>i, j</sup>, Luis Gales<sup>b, c, e</sup>, Jordi Llop<sup>k</sup>, Jordi Quintana<sup>d, 1, \*\*</sup>, Isabel Cardoso<sup>b, c, e, 2, \*\*\*</sup>, Gemma Arsequell<sup>a, 2, \*</sup>

<sup>a</sup> Institut de Química Avançada de Catalunya (I.Q.A.C.-C.S.I.C.), E-08034, Barcelona, Spain

<sup>b</sup> IBMC - Instituto de Biologia Molecular e Celular, PT-4200-135, Porto, Portugal

<sup>c</sup> I3S - Instituto de Investigação e Inovação em Saúde, Universidade do Porto, PT-4200-135, Porto, Portugal

<sup>d</sup> Plataforma Drug Discovery, Parc Científic de Barcelona (PCB), E-08028, Barcelona, Spain

<sup>e</sup> Instituto de Ciências Biomédicas Abel Salazar (ICBAS), PT-4050-013, Porto, Portugal

<sup>f</sup> Facultat de Farmàcia i Ciències de l'Alimentació, University of Barcelona, E-08028, Barcelona, Spain

<sup>g</sup> Institut Químic de Sarrià, Universitat Ramon Llull, E-08017, Barcelona, Spain

<sup>h</sup> Centres Científics i Tecnològics, Universitat de Barcelona, E-08028, Barcelona, Spain

<sup>i</sup> CIC bioGUNE, Basque Research and Technology Alliance (BRTA), Bizkaia Technology Park, Building 800, E-48160, Derio, Spain

<sup>j</sup> Ikerbasque, Basque Foundation for Science, E-48009, Bilbao, Spain

<sup>k</sup> CIC biomaGUNE, Basque Research and Technology Alliance (BRTA), E-20014, San Sebastian, Spain

## ARTICLE INFO

## Article history:

Received 13 August 2021

Received in revised form

8 September 2021

Accepted 9 September 2021

Available online 14 September 2021

## Keywords:

Targeting transthyretin

Small molecule chaperones (SMCs)

Alzheimer's disease drug discovery

Transthyretin tetramer stability

Transthyretin

A $\beta$  interaction

HTS screening

Protein-protein interactions

Repurposing

Multi-target screening

Computational screening

Alzheimer's disease (AD)

AD disease-modifying drugs

## ABSTRACT

Transthyretin (TTR) has a well-established role in neuroprotection in Alzheimer's Disease (AD). We have setup a drug discovery program of small-molecule compounds that act as chaperones enhancing TTR/Amyloid-beta peptide (A $\beta$ ) interactions. A combination of computational drug repurposing approaches and *in vitro* biological assays have resulted in a set of molecules which were then screened with our in-house validated high-throughput screening ternary test. A prioritized list of chaperones was obtained and corroborated with ITC studies. Small-molecule chaperones have been discovered, among them our lead compound Iododiflunisol (IDIF), a molecule in the discovery phase; one investigational drug (luteolin); and 3 marketed drugs (sulindac, olsalazine and flufenamic), which could be directly repurposed or repositioned for clinical use. Not all TTR tetramer stabilizers behave as chaperones *in vitro*. These chemically diverse chaperones will be used for validating TTR as a target *in vivo*, and to select one repurposed drug as a candidate to enter clinical trials as AD disease-modifying drug.

© 2022 The Authors. Published by Elsevier Masson SAS. This is an open access article under the CC BY license (<http://creativecommons.org/licenses/by/4.0/>).

\* Corresponding author.

\*\* Corresponding author.

\*\*\* Corresponding author. IBMC - Instituto de Biologia Molecular e Celular, PT-4200-135, Porto, Portugal.

E-mail addresses: [jordiramon.quintana@upf.edu](mailto:jordiramon.quintana@upf.edu) (J. Quintana), [icardoso@ibmc.up.pt](mailto:icardoso@ibmc.up.pt) (I. Cardoso), [gemma.arsequell@iqac.csic.es](mailto:gemma.arsequell@iqac.csic.es) (G. Arsequell).

<sup>1</sup> Present Address: Dr. Jordi Quintana, Research Programme on Biomedical Informatics, Universitat Pompeu Fabra (UPF), Barcelona, Spain.

<sup>2</sup> Equally contributing corresponding authors

## 1. Introduction

Alzheimer's disease (AD) is a progressive neurodegenerative disease and is the leading cause of dementia. AD is characterized by accumulation of amyloid- $\beta$  ( $A\beta$ ) aggregates in various conformations, filamentous intraneuronal inclusions mainly constituted by hyperphosphorylated Tau protein (p-Tau), and synaptic dysfunction and neuronal loss [1].

One of the most difficult challenges in AD research is to find a disease modifying therapy (DMT), this is, a therapy with an agent that produces an enduring change in the clinical progression of AD, by changing the biology of AD and producing neuroprotection by interfering in the underlying pathophysiological mechanisms of the disease process that lead to cell death (often through a variety of intermediate mechanisms such as effects on amyloid or tau) [2]. The five drugs available in the market for AD are involved in only improving symptoms and are highly patient dependent. Aduhelm (aducanumab) [3,4], by Biogen and Eisai, an antibody that targets amyloid-beta, was approved in June 2021 by the US Food and Drug Administration (FDA) under its accelerated approval pathway. FDA approval of Aduhelm, the first drug with a putative disease-modifying mechanism for AD treatment, has been met with a fair degree of skepticism and controversy [5,6]. No other putative disease modifying drugs or new symptomatic treatments for AD have achieved regulatory approval since 2003 [7]. There are 126 agents in the current AD treatment pipeline, 28 of them in phase III, 74 in phase II and 24 in phase I clinical trials. The majority of drugs in trials (82.5%) target the underlying biology of AD with the intent of disease modification [8].

AD drug development is not delivering new drugs in the last decades. Among the many explanations for such failure, one is the lack of new chemical entities from drug discovery approaches that reach the clinical phase I level [9–12]. There is an urgent need to find a treatment that prevents, delays the onset or slows the progression of this devastating disease.

With the aim of contributing with new candidate drugs that, after preclinical tests, may feed the currently exhausted pipeline of drugs in phase I for AD, we have settled a drug discovery program targeting transthyretin (TTR) and searching for small-molecule chaperones that may improve the neuroprotective function of TTR in AD.

Transthyretin (TTR), a homotetrameric protein mainly synthesized by the liver and the choroid plexus (CP), and secreted into the blood and the cerebrospinal fluid (CSF), respectively, has been specially recognised for its functions as a transporter protein of thyroxine ( $T_4$ ) and retinol [13]. The importance of TTR has also been robustly established in AD pathogenesis [14]. It is most remarkable that TTR is the main  $A\beta$  binding protein in the CSF.[15–17] This binding is believed to naturally prevent  $A\beta$  aggregation and toxicity in this media. Comparative analysis of TTR evidenced decreased levels of this protein, not only in the CSF [18,19] but also in plasma [20–22] of AD patients, compared to controls. AD TTR-hemizygous mice showed increased  $A\beta$  production and deposition, compared to AD TTR WT littermates [23], whereas overexpressing human TTR WT in an AD mouse model decreased neuropathology and  $A\beta$  deposition [24]. Regarding the mechanisms proposed as underlying TTR neuroprotection in AD, *ex vivo* and *in vitro* studies, established that TTR has the ability to bind to  $A\beta$ , avoiding its aggregation and toxicity [25–30]. Recent reports suggest that TTR binds to  $A\beta$  oligomers and inhibits primary and secondary nucleation processes [29,30]. TTR was also shown to assist  $A\beta$  brain efflux through the blood-brain barrier, and to promote its degradation in the liver. Results also revealed that TTR regulates the expression of LRP1, by increasing its levels, both in the brain and in the liver [31]. Recent data implicated TTR reduction in the thickening of the basement

membrane of brain microvessels in AD mice,[32] an alteration that also occurs in the AD brain [33].

TTR tetrameric stability appears as a key factor in its interaction with  $A\beta$  peptide. Interestingly, TTR stability is also a key factor in Familial Amyloid Polyneuropathy (FAP) [34,35] a systemic amyloidosis with a special involvement of the peripheral nerve system, which results from the aggregation, deposition and toxicity of mutated TTR. Since it is believed that tetramer dissociation into monomers is the first step leading to TTR amyloid formation [36], TTR tetrameric stabilization has been defined as the basis for one of the possible therapeutic strategies in FAP [37–39]. Such stabilization can be achieved through the use of small compounds sharing molecular structural similarities with thyroxine ( $T_4$ ) which bind in the  $T_4$  central binding channel [40,41]. The search for TTR stabilizing ligands using virtual screening and computational procedures has been carried out previously [42–44] and there is a large number of TTR and TTR-ligand three dimensional structures reported at the PDB [45]. These computational and structural studies have been instrumental in the design, discovery and development of TTR stabilizing compounds that have either reached the market, like Tafamidis [46,47], or that have reached clinical phases, like Tolcapone, a repurposed drug approved for the treatment of Parkinson's disease (Fig. 1) [48].

We have demonstrated by early *in vitro* studies that TTR and  $A\beta$  bind together and that this interaction can be enhanced by a small set of TTR tetramer-stabilizing compounds [49], one of them Iododiflunisal (IDIF), a iodinated analog of the NSAID diflunisal (DIF) (Fig. 1) [50–52]. More importantly, *in vivo* administration of IDIF to a mouse model of AD, resulted in decreased brain  $A\beta$  levels and deposition [53,54], and improving the cognitive functions that are impaired in this AD-like neuropathology [53].

Drug repurposing of already known drugs for new indications is a drug discovery approach increasingly being used to search for new therapies for diseases with unmet clinical needs. Both *in silico* [55,56] and experimental [57] approaches on drug repurposing have been recently reviewed, as well as the application of this approach to drug discovery for AD [58–60]. Furthermore, another interesting strategy in drug discovery is the multi-target approach, which aims to have a synergistic effect thanks to the interaction of a given ligand with different targets that are involved in a disease's pathway. Therefore, these synergies through target promiscuity could be translated into lower doses and reduced side effects [61,62].

In this paper, we report the discovery of TTR stabilizers through two complementary *in silico* drug repurposing approaches, as well as the systematic biological evaluation of the selected compounds on TTR stability, through competition with  $T_4$  for TTR binding, and by measuring the amount of monomers. This process has led to the prioritization of a set of 53 TTR tetramer stabilizing compounds and to an analysis of their ability to enhance the TTR/ $A\beta$  interaction. Using our in-house validated high-throughput screening (HTS) ternary assay [28], we have evaluated these 53 small-molecule compounds and have obtained a subset of small molecule chaperones (SMCs), among them our lead compound IDIF, one clinical phase compound (luteolin), and three approved drugs for other diseases (sulindac, olsalazine and flufenamic acid), that could enter clinical trials for AD as repurposed drugs.

## 2. Results and discussion

**Computational studies.** In order to find small molecule chaperones that enhance the TTR/ $A\beta$  interaction, two computational pipelines have been established, addressing drug repurposing and polypharmacology, as shown in Fig. 2. The first approach started with the construction of a TTR/ $A\beta$  model [63] as described in the

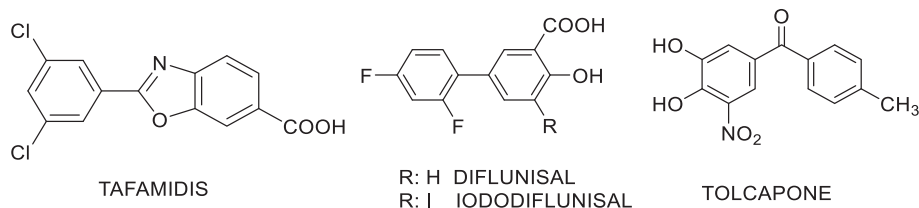


**Fig. 1.** Chemical structures of TTR tetramer stabilizers: the orphan drug Tafamidis, the Non-steroidal anti-inflammatory drug (NSAID) diflunisal (DIF), the repurposed drug Tolcapone for Familial amyloid polyneuropathy (FAP) and our lead compound Iododiflunisal (IDIF).

Experimental Section. Then, compounds from the Integrity database (<https://integrity.clarivate.com/integrity/xmlxsl/>) and from the literature were selected, so as they were either (i) known TTR binders, (ii) amyloid peptide binding ligands, or (iii) both, or (iv) compounds under study in clinical phases for the treatment of Alzheimer's disease. The use of the CARLSBAD software and database [64] allowed us to find privileged scaffolds with reported biological activity against both TTR and A $\beta$  systems. This scaffold hunting methodology allowed us to find a group of compounds containing the stilbene substructure and able to interact with both entities (TTR and A $\beta$ ). Then, this stilbene scaffold was used to select molecules by substructure search in the Integrity-derived and literature-derived databases already mentioned, and the selected compounds were then prioritized by docking into our TTR/A $\beta$  model [63]. In total, 48 compounds with docking scores similar to IDIF (used as the cross-reference compound in the docking experiments) were prioritized, and 20 of them, that were commercially available, were selected and acquired to carry out the experimental assays.

A second computational approach was carried out in order to exploit the drug-promiscuity and polypharmacology in a multitarget-based pipeline. This methodology allowed us to identify molecules able to bind TTR that also bind additional targets that have been associated with the treatment of AD and that are relevant in its pathological pathways. As described in the Experimental section, this strategy includes multi-target molecular docking and molecular searches through common pharmacophore models to a set of targets (Fig. 2B). Starting from the Integrity database (<https://integrity.clarivate.com/integrity/xmlxsl/>), which contains small molecules and drugs in the market or advanced clinical phases, we selected nearly 1400 compounds that were reported in preclinical, clinical or marketed phase and that had their protein target reported as one or more of the following, which have been associated to AD: APP (amyloid precursor protein); AchE (acetylcholinesterase); IL-10 (interleukin-10);  $\alpha$ -,  $\beta$ - and  $\gamma$ -secretases; Tau protein; GABA and glutamate receptors. All these compounds were then docked into the TTR model, prioritizing a pool of 134 molecules that would theoretically bind the TTR T<sub>4</sub>-channel with an affinity similar to IDIF. These molecules were then analyzed theoretically through cross-docking into the following protein structures: IL-10 (Interleukin-10) (PDB code 1ILK); inhibitor domain of APP (amyloid beta-protein precursor) (PDB code 1AAP);  $\beta$ -secretase (memapsin 2) complexed with inhibitor OM99-2 (PDB code 1FKN); human acetylcholinesterase (AChE) complexed with fasciculin-II (PDB code 1B41); metabotropic glutamate receptor 1 with LY341495 antagonist (PDB code 3KS9); metabotropic glutamate receptor 5 with glutamate (PDB code 3LMK). All these docking experiments lead to a prioritized list of 85 molecules, which were filtered to 27 molecules that would theoretically bind to TTR/A $\beta$  complex (by docking experiments) and 4 additional AD related targets (multi-target docking approach for ligand selection). In addition, the 134 molecules that were selected before through docking with TTR were further analyzed computationally through the software

LigandScout [65]. A common pharmacophore was built starting from the binding sites of TTR,  $\beta$ -secretase, metabotropic glutamate receptor 1 and metabotropic glutamate receptor 5, and then the 134 molecules were screened against this pharmacophore; 13 of them coincided with the list of 27 molecules derived from the multi-target docking, but we were able to select 4 additional molecules that matched with the common pharmacophore. The Table S1 in the Supporting Information contains all the chemical structures of the compounds that were selected through these computational procedures, as well as other molecules (that had been reported as TTR ligands, in the literature, and from previous studies in our laboratory), which were also selected after docking them into our TTR/A $\beta$  model, and the results of the associated experimental assays for all the selected molecules, which are described hereunder.

**Thyroxine binding assays and TTR stability assays.** To confirm the ability of the proposed compounds to bind TTR we designed a flow chart through which all the selected compounds were experimentally assayed (Fig. 3).

The first assay, to which all compounds were submitted, was a T<sub>4</sub> displacement assay [48,50]. In brief, radiolabeled [<sup>125</sup>I]-T<sub>4</sub> was incubated alone or in the presence of each of the compounds with TTR, and then samples were run in a native PAGE gel. Compounds that are able to bind to TTR in the T<sub>4</sub> central binding channel, and thus to displace [<sup>125</sup>I]-T<sub>4</sub>, result in decreased intensity of the [<sup>125</sup>I]-T<sub>4</sub>/TTR band. When using plasma as a source of TTR, which is the case of the present work, this approach also enables the visualization of the bands corresponding to the other T<sub>4</sub> transporter proteins, such as thyroxine-binding globulin (TBG) and albumin. IDIF was used as a reference compound (see representative example in Fig. 3A). This assay, although not quantitative, is of utmost importance, in particular when using human plasma, since it also reveals the effect of the compounds in the other referred T<sub>4</sub> transporter proteins, and therefore, on their specificity for TTR binding. Using this approach, we characterized the behavior of the compounds regarding their ability to displace T<sub>4</sub> and their specificity for TTR binding (see Table S1 in the Supporting Information for a complete view of the behavior of all compounds in the qualitative T<sub>4</sub> displacement assay).

In addition to high affinity for TTR, compounds should also be specific for this protein, since lack of specificity, together with the high abundance of other plasma proteins, such as albumin, for instance, could lead to failure in therapeutics. However, at this stage of our selection, we mainly aimed at identifying strong TTR stabilizers which will be further investigated for their capacity to enhance the TTR/A $\beta$  interaction. Thus, at this point all compounds that completely or significantly displaced T<sub>4</sub> from TTR, were selected for the quantitative assay regardless of their specificity (Table S1). Selected compounds were then evaluated in a quantitative T<sub>4</sub> assay to determine their EC<sub>50</sub> and values were compared to the EC<sub>50</sub> of T<sub>4</sub> (a representative example is given in Fig. 3B, results in Table S2). Analysis of results enabled us to conclude that only compounds that showed complete T<sub>4</sub> displacement in the

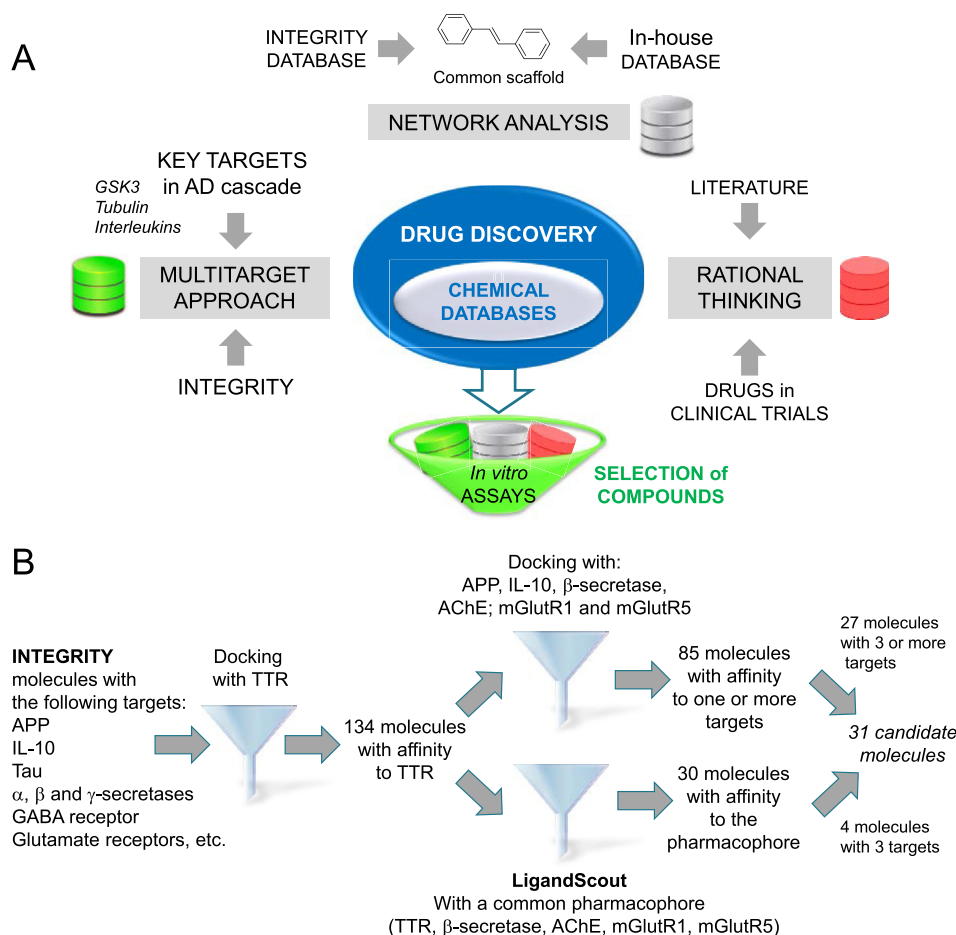


**Fig. 2.** Computational workflows for the selection of modulators of TTR/A $\beta$  interaction (A) Based on drug repurposing and multi-target approach; (B) Based on multi-target computational docking and searches on common pharmacophores for several targets.

qualitative assay, produced EC<sub>50</sub> T<sub>4</sub>/EC<sub>50</sub> compound ratios higher than 1, *i.e.*, with affinity to TTR higher than the one of T<sub>4</sub>. Nevertheless, a ratio of EC<sub>50</sub> T<sub>4</sub>/EC<sub>50</sub> compound of 0.5 or superior was used to identify a pool of compounds able to bind TTR efficiently and therefore those that should be tested in our proprietary HTS ternary assay [28]. In some instances, compounds revealed a non-standard or ambiguous behavior, hindering the statistical analysis performed for the rest of the compounds.

Nonetheless, and in order to avoid elimination of compounds that could stabilize TTR by pathways other than binding to the T<sub>4</sub> binding site, all of the non-selected compounds were assessed in a TTR stability assay [66]. This approach was employed to test and to evaluate the ability of the non-selected compounds to stabilize TTR, by electrophoretic means, under semi-denaturing conditions, as described in the Experimental section. As readout, we assessed the levels of monomeric TTR upon incubation with each compound and values were compared to those obtained in the absence of compound.

Fig. 3C displays representative results obtained in this stability assay showing different levels of the TTR monomer. The graphic represents the intensity of the monomer band, considering the value of 1 for the control. Compounds that reduced the intensity of the monomer band to at least half of the intensity in the control, were considered for the final list of the compounds to enter a future ternary assay (Table S1).

Altogether, compounds selected from the T<sub>4</sub> quantitative and the TTR stability assays constitute a subset of 53 molecules

amenable to be screened using our proprietary HTS ternary assay (Table S4 in the Supporting Information).

**Crystal structures of TTR:ligand complexes.** From this final list of compounds to enter a future ternary assay, two compounds, **35** and **73**, were selected for the structure elucidation of the TTR complexes by X-ray diffraction, because their TTR-ligand structures have not been previously analyzed (Table S3 in Supporting Information). Both compounds bind in the so-called thyroxine binding sites (Fig. 4). Compound **35** (Fig. 4, left panel) binds very deeply with the iodinated ring located at the outmost part of the T<sub>4</sub> channel. This binding induces the rotation of Ser117 side chains of the four monomers creating new strong intermonomer hydrogen bonds between these residues. The Lys15 residues, located at the entrance of the binding sites, establish interactions with the carboxylate substituents of the ligand. Compound **73** does not bind so deeply in the channel as **35** (Fig. 4, right panel) and, consequently, it does not induce the formation of such strong interactions between the Ser117 residues of the TTR tetramer. The Lys15 residues, in the TTR: **73** complex, are not pointing to the center of the channel and are not involved in interactions with the compound.

**Selection of small-molecule chaperones (SMCs): HTS ternary assay, ITC studies and ThT assays.** To efficiently screen for potential small-molecule chaperones of the TTR/A $\beta$  interaction, we have used our recently in house developed and validated high-throughput assay that relies on the ability of the test compounds to prevent A $\beta$  aggregation in solutions of preformed TTR/A $\beta$

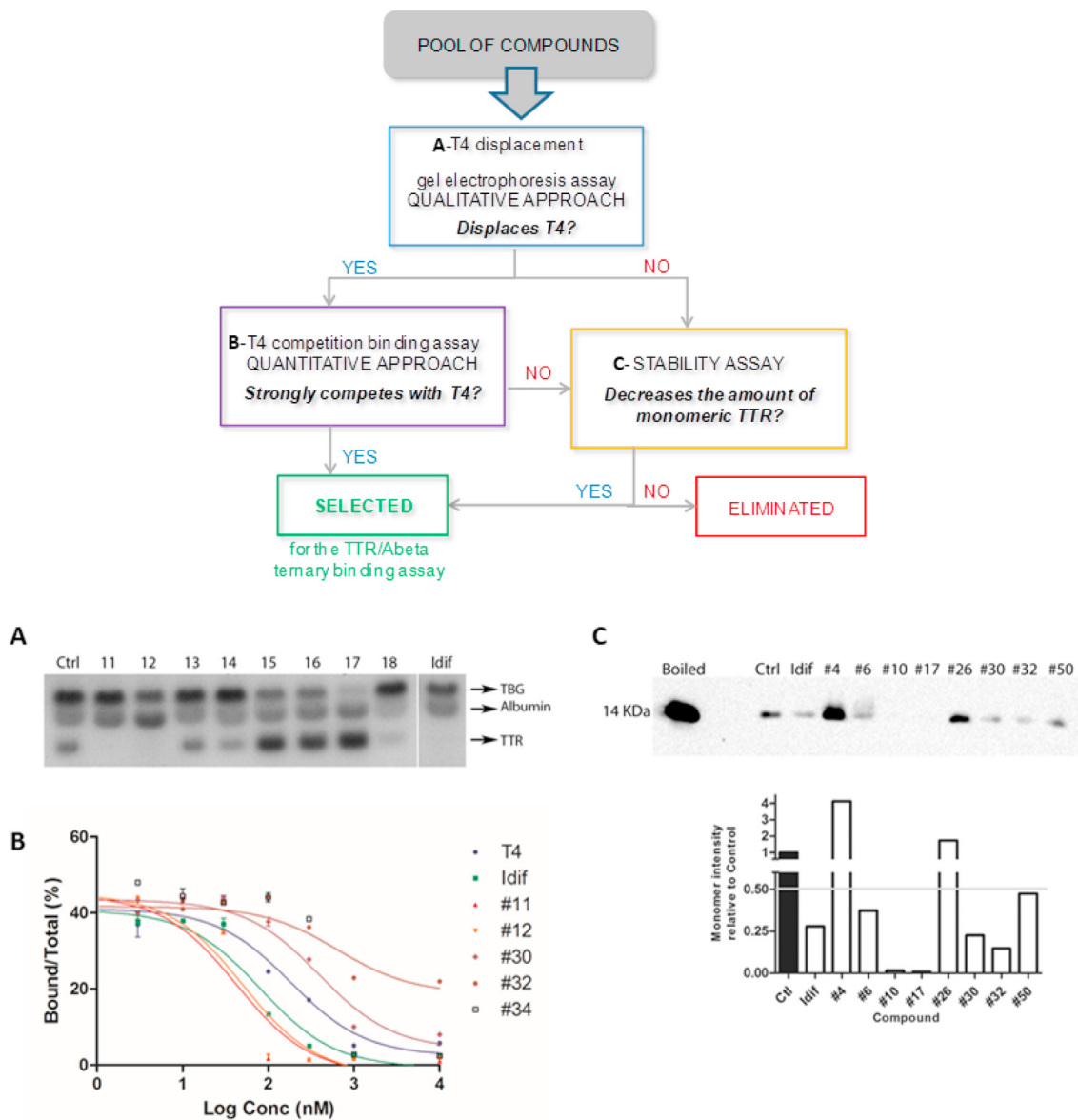


**Fig. 3.** Flowchart to which compounds were subjected to determine experimentally which compounds bind to and stabilize TTR, and representative images of the results obtained in each assay. (A) The  $T_4$  binding gel electrophoresis assay, using human plasma incubated with  $[^{125}I]$ - $T_4$  and with various compounds as competitors. The migration of the different plasma  $T_4$  binding proteins is indicated. (B) The displacement of  $[^{125}I]$ - $T_4$  from WT TTR by competition with the compounds. The curves were obtained using various compounds indicated as competitive inhibitors. (C) The TTR stability assay, in which samples were analyzed by Western Blot after incubation of the compounds with WT-TTR, under semi-denaturing conditions; the quantification plot presents the intensity of monomer band, relative to the control condition which was considered one. (See compounds in Table S1 at the SI).

complexes [28]. The assay makes use of  $A\beta(12-28)$  which has analogous properties as full length  $A\beta$  peptides but is a less expensive and more stable peptide. Thus, the recombinant wtTTR is incubated with the test compound (ratio TTR/compound 1:2) during 1 h and then,  $A\beta(12-28)$  is added to the complex and UV monitoring of turbidity for 6 h allows to determine its potency. A complete high-throughput screening in this ternary assay was carried out for all the 53 compounds previously selected from computational and biological studies (see Fig. S1 and Table S5 in the Supporting Information).

After classifying the compounds according to their potency at reducing  $A\beta$  aggregation a prioritized list was obtained (See Fig. 5). In this list we found our lead compound IDIF, the natural product luteolin (LUT), a compound in clinical phases, and three registered

drugs, olsalazine (OLS), sulindac (SUL) and flufenamic acid (FLU), among others (See Fig. 5C).

Furthermore, Isothermal Titration Calorimetry (ITC) technique has been used to corroborate the chaperoning effect of five of the best small-molecule compounds as described previously [27]. Thus, we have compared the binding in the  $A\beta(12-28)/TTR/SMC$  ternary complexes with the binary interaction  $A\beta(12-28)/TTR$  (Figs. S12 and S13 at the Supporting Information). In addition, a full thermodynamic characterization of the ternary complexes with  $A\beta(1-40)$  and TTR and each of the five best selected SMCs was obtained (Fig. 6). The binary TTR/ $A\beta(1-40)$  (1:1) complex formation shows a dissociation constant of  $K_d = 6.49 \mu M$ . However, IDIF enhances this interaction between TTR and  $A\beta(1-40)$ , since the  $K_d$  is reduced to  $3.34 \mu M$  when TTR in the presence of IDIF is titrated

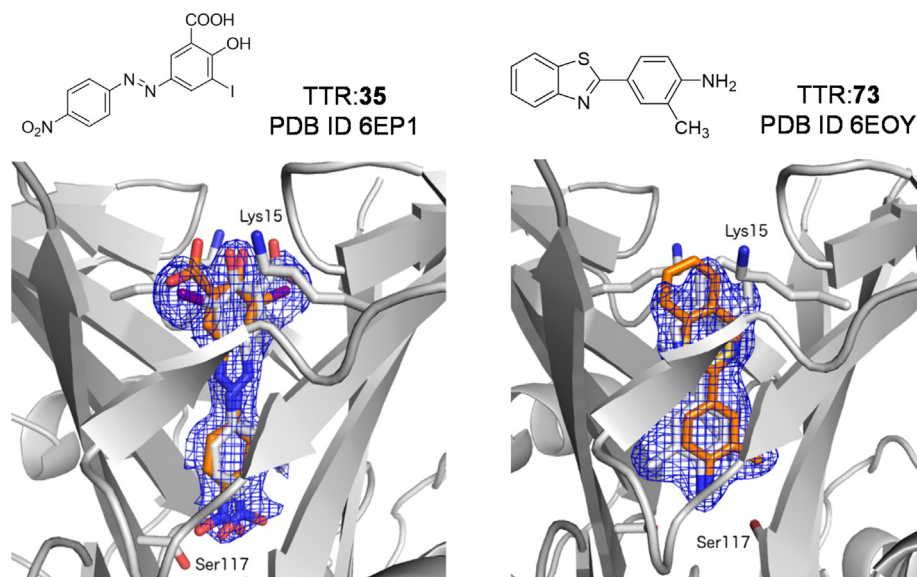


**Fig. 4.** Close view of one binding site of the crystal structures of TTR:**35** (left, PDB ID 6EP1) and TTR:**73** (right, PDB ID 6EOY). The two-symmetry related positions of each compound are shown with carbon atoms in grey and orange. The 2Fo-Fc electron density maps at  $1\sigma$  are drawn as a blue mesh around compounds **35** and **73** and residues Lys15 and Ser117 highlighted in stick representation.

with A $\beta$ (1–40). Similar improvements were observed for the ternary complexes with the best SMCs (*i.e.* K<sub>d</sub> = 1.52  $\mu$ M (LUT); 3.42  $\mu$ M (SUL); 0.81  $\mu$ M (OLS) and 2.34  $\mu$ M (FLU)).

To complement the results gathered so far, we performed the aggregation kinetics of A $\beta$ (1–42) in the presence of the five selected SMCs using by ThT assays, obtaining coherent results with the turbidity measurements observed with A $\beta$ (12–28) (Fig. 7). Interestingly, none of the best small molecule chaperones interfered with the aggregation kinetics of A $\beta$ (1–42) (Figs. S2–S11). Additionally, we have performed dose-response studies on the binary interaction TTR/A $\beta$  (Fig. 7B) and in the ternary interaction when TTR is complexed with IDIF (Fig. 7C). As shown in Fig. 7C the aggregation kinetics of A $\beta$ (1–42) in the presence of TTR complexed with IDIF are concentration dependent of this small-compound.

Mounting evidence has demonstrated that A $\beta$  peptides and their oligomeric forms are toxic to neural cells leading to apoptosis and cellular death. It is also well established that TTR protects against this neurotoxicity [25,29,30]. To evaluate A $\beta$ -induced neuronal apoptosis in the presence of TTR stabilized by the selected SMCs, we evaluated caspase 3 activation in SH-SY5Y cells. We confirmed that TTR prevented the noxious effect of A $\beta$ (1–42) peptide, reducing significantly the levels of caspase-3 activation, as compared to those produced by the oligomers. Also, as we previously reported [28], TTR stabilized by IDIF was even more potent at protecting against A $\beta$  toxicity, as caspase 3 levels were significantly reduced when compared to those generated in cells treated with A $\beta$ (1–42) co-incubated with TTR (without IDIF). Importantly, the effect of flufenamic acid (FLU), olsalazine (OLS), and luteolin (LUT) was found to be similar to that of IDIF. Sulindac (SUL), while promoting the protection conferred by TTR, was not as strong as the other tested compounds (Supporting Information, Fig. S14).

The blood-brain barrier (BBB) is one of the bottlenecks in brain drug development and is the single most important factor limiting the future growth of neurotherapeutics [67]. In our previous papers we have shown that BBB penetration is facilitated by the binding of IDIF to TTR [53,54,68]. Importantly, the BBB penetration ability of some of our selected compounds has been previously reported in the literature [69–71]. Here, we have also analyzed *in silico* the molecular properties of the 5 selected compounds, and results

predict that they cross the BBB (See Supporting Information) [72,73].

Altogether, these results confirm that TTR is a neuroprotective protein, preventing A $\beta$  toxicity, and that TTR performance can be enhanced by small-molecule chaperones of the TTR/A $\beta$  interaction, prompting TTR stabilization as a promising therapeutic strategy in AD.

### 3. Conclusions

In this paper, we have first taken a combined computational/experimental approach to select a pool of chemically diverse compounds, that may enhance the ability of TTR to sequester the A $\beta$  peptide. In order to carry out this comprehensive study, two complementary computational procedures were used: a) drug repurposing through virtual screening and pharmacophore searches, starting from a large set of compounds that have either reached the market or are in clinical phases, and docking them into our built TTR/A $\beta$  molecular model; and b) a multi-target approach, where we selected molecules that were theoretically interacting with our built TTR/A $\beta$  molecular model, but also would theoretically interact with a group of four protein targets that have been associated with AD.

All of the selected compounds that underwent these computational procedures, and other known TTR ligands, were sequentially assayed in a screening cascade covering TTR binding through both a T<sub>4</sub> displacement assay (qualitative) and a TTR – T<sub>4</sub> competition assay (quantitative), followed by a TTR stabilizing assay.

The combined virtual and experimental screening approach has led to 53 highly diverse compounds that strongly stabilize TTR. Among these compounds, compound 35 and the drug olsalazine had not been previously described as TTR stabilizers and may be relevant for TTR-related therapies.

Of note, these 53 compounds were good candidates for the analysis of the modulation of the TTR/A $\beta$  interactions, and they were analyzed through our robust HTS ternary assay. The results of this ternary assay show a prioritized list of small molecule chaperones (SMCs) of the TTR/A $\beta$  interaction providing the basis for a novel therapeutic target for Alzheimer's disease (AD). Among the

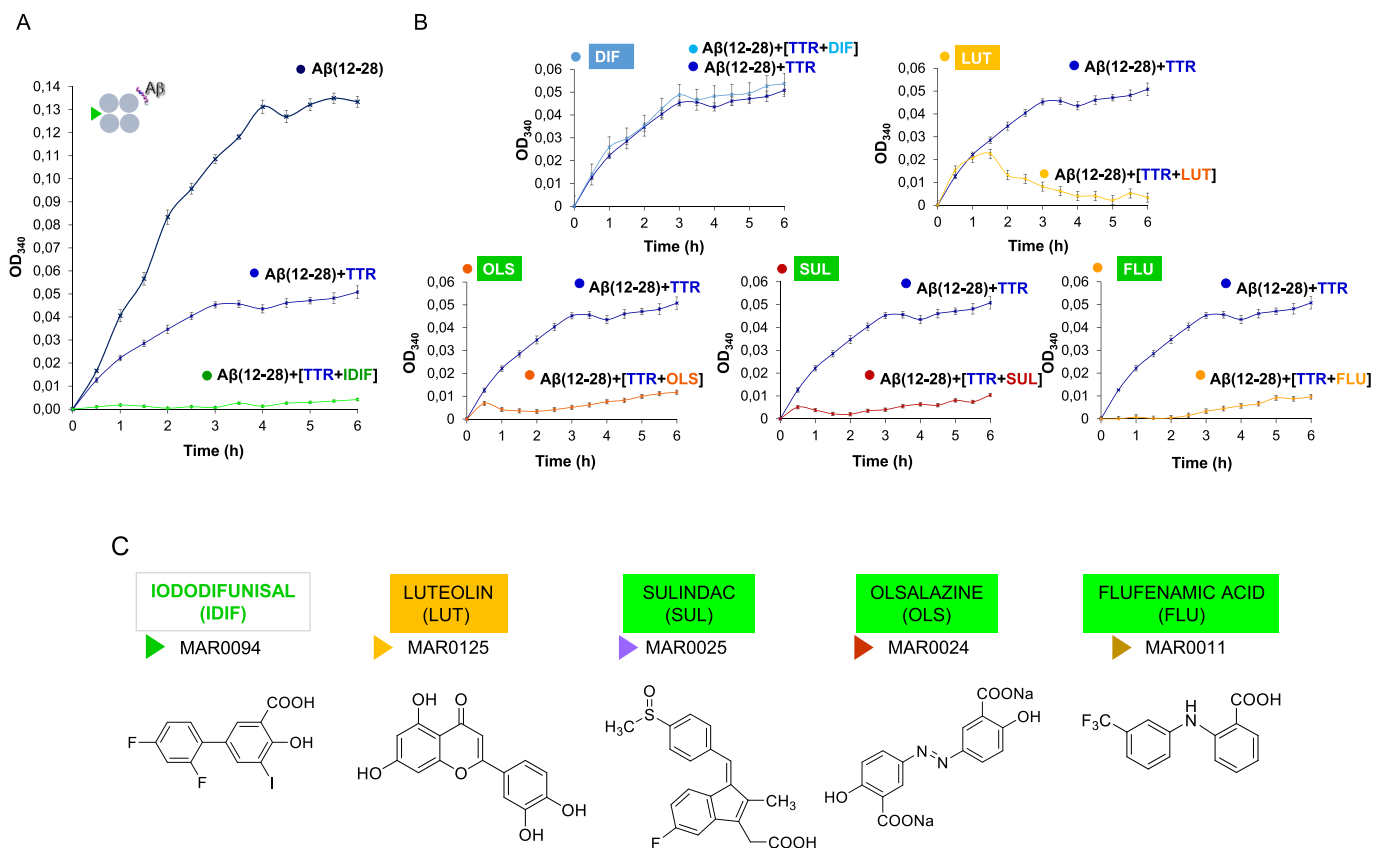


**Fig. 5.** HTS assays. Kinetics of aggregation with best chaperones: (A) binary [Aβ(12–28) + TTR] and ternary interactions [Aβ(12–28) + (TTR+IDIF)]; (B) binary [Aβ(12–28) + TTR] and ternary interactions [Aβ(12–28) + (TTR+SMC)] with SMCs: LUT, SUL, OLS, and FLU. Ternary interactions [Aβ(12–28) + (TTR+DIF)] are added for comparison purposes. (C) Chemical structures of the best chaperones (IDIF, LUT, SUL, OLS, and FLU).

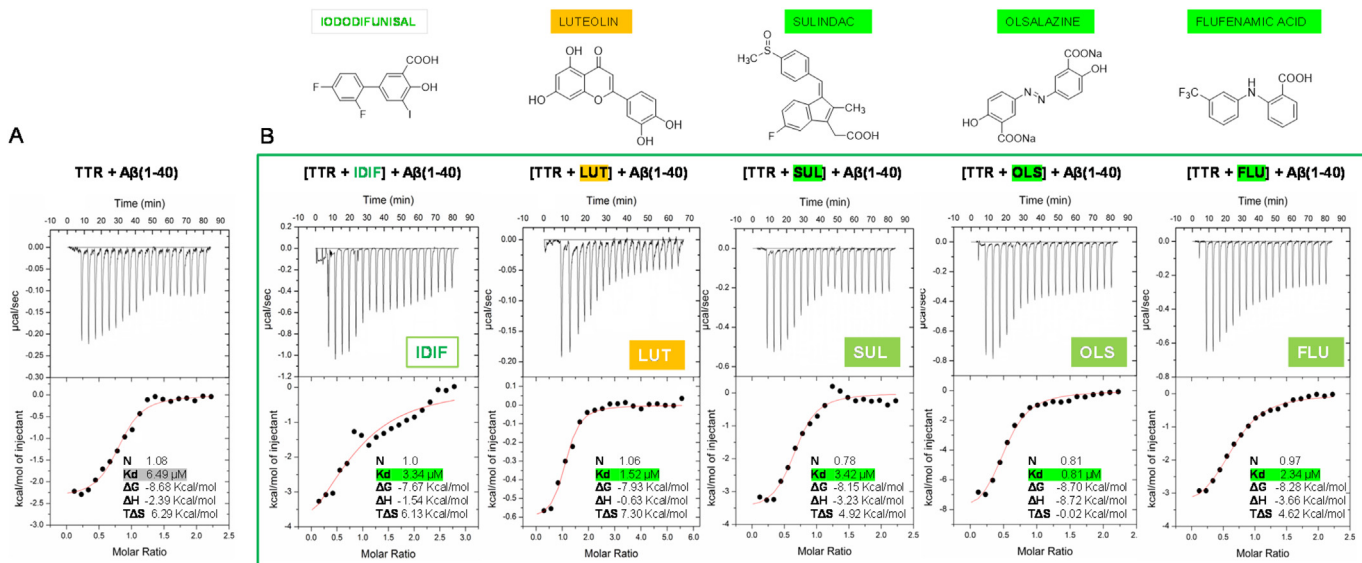


**Fig. 6.** ITC studies of the: (A) binary Aβ(1–40)/TTR complex; and (B) of the ternary complexes Aβ(1–40)/(TTR/SMC) (SMC: IDIF, LUT, SUL, OLS AND FLU).

SMCs, we have found small-molecules as our lead small-molecule compound IDIF which is one of the best SMCs, and also three marketed drugs (olsalazine, sulindac, and flufenamic acid) and one investigational drug (luteolin), which could be directly repurposed or repositioned for clinical use. The orphan drug Tafamidis and the repurposed Parkinson's drug Tolcapone have been reported to be

excellent TTR tetramer stabilisers, but these drugs have no chaperoning effect in our *in vitro* assays, showing that not all good TTR tetramer kinetic stabilisers are good SMCs.

Our drug discovery program offers the possibility to explore the chemical space by HTS of commercially available libraries of drugs/compounds to find new SMCs. Further work will be carried out to

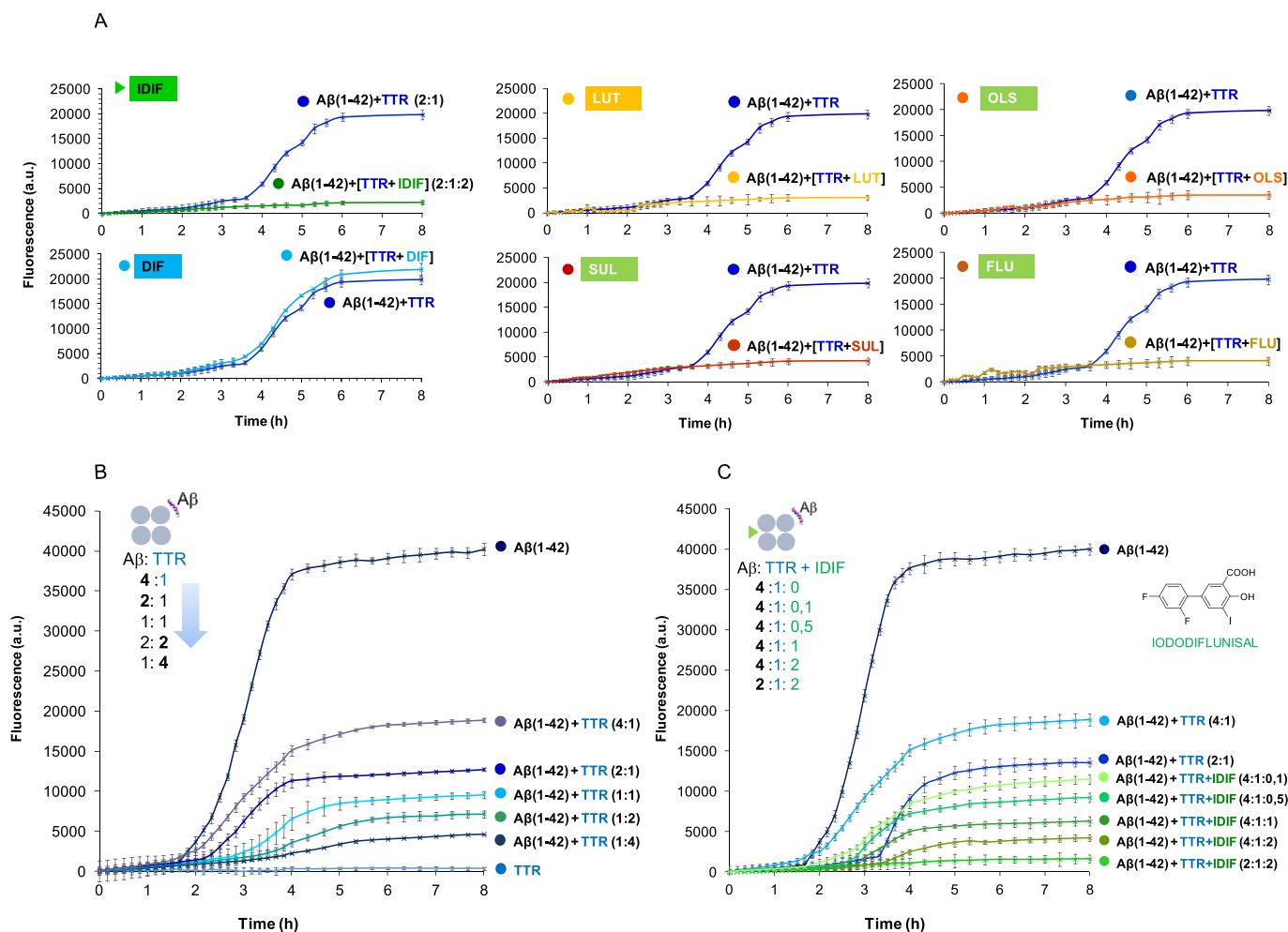


**Fig. 7.** Aggregation kinetics of Aβ(1-42) monitored by ThT fluorescence assays: (A) Binary interactions [Aβ(1-42) + TTR] at a ratio (2:1) and ternary interactions [Aβ(1-42) + (TTR+SMC)] at a ratio (2:1:2) for five SMCs (IDIF, LUT, SUL, OLS, and FLU) and ternary interaction [Aβ(1-42) + (TTR+DIF)], for comparison purposes; (B) Dose/response studies: kinetics of aggregation of Aβ(1-42) in the presence of TTR at different ratios from (4:1) to (1:4); and (C) Dose/response studies: kinetics of aggregation of Aβ(1-42) in the presence of (TTR+IDIF), fixed ratio Aβ(1-42)/TTR to (4:1) and increasing the ratio of TTR/IDIF from (1:0) to (1:2).

explore the activity of some chemical scaffolds such as the biphenyl one present in IDIF, so as to build structure-activity relationships from the HTS ternary assay results. In particular, the SMC IDIF will be optimized for ADME properties and to improve blood-brain barrier (BBB) passage.

A small set of these SMCs will be prioritized to enter preclinical safety studies, analyzing their *in vivo* behavior, in order to select one repurposed drug as a candidate to enter clinical trials for AD.

These selected small-molecule chaperones provide the basis for a novel target for Alzheimer's disease, based on targeting trans-thyretin. We envisage that this new target will feed the currently exhausted pipeline of drugs in phase I for AD with the goal of increasing AD disease-modifying therapies. In addition, the three marketed drugs reported in this work as SMCs of the TTR/Aβ interaction (sulindac, olsalazine and flufenamic acid) could directly enter a clinical phase program as candidate AD therapies, as an example of drug repurposing.

#### 4. Material and methods

**General procedure for molecular models preparation.** A molecular model of TTR was generated using the three-dimensional coordinates of the TTR protein structure (PDB code 1DVQ), available at the Protein Data Bank (PDB) ([www.rcsb.org](http://www.rcsb.org)).

For hydrogen atoms refinement and energy minimization, the Protonate 3D package implemented in MOE 2015.10 was employed to add hydrogen atoms to TTR which were further submitted to an energy-minimization process [74]. Partial charges were obtained by computing the electrostatic potentials in the optimized structures. The energy minimization step was carried out using a distance-dependent dielectric constant and a cut-off distance of 10 Å for the van der Waals interactions. In the final step, the refinement was accomplished using 1000 cycles of steepest descents followed by conjugate gradients until the maximum gradient of the energy was smaller than 0.05 kcal/mol Å<sup>2</sup>.

The same procedure and parameters were used to compute the following proteins used in this work: IL-10 (interleukin-10) (PDB code 1ILK); inhibitor domain of APP (amyloid beta-protein precursor) (PDB code 1AAP); β secretase with inhibitor OM99-2 (PDB code 1FKN); human acetylcholinesterase with Fasciculin-II (PDB code 1B41); metabotropic glutamate receptor 1 with LY341495 antagonist (PDB code 3KS9); metabotropic glutamate receptor 5 with glutamate (PDB code 3LMK).

**Docking experiments (TTR/Aβ computational model) procedure.** The MOE 2015.10 package [74] was used to perform the docking studies between the refined TTR X-Ray crystallographic structure (as template) and Aβ peptide (as ligand). Alpha Triangle was used as placement method; Alpha HB as score function, and



AMBER10 as force-field [75] in the first refinement step of the docking solutions. A rescoring step was also implemented in this computational pipeline, using London DG as function score, and again AMBER10 as forcefield for the last refinement step of this docking study.

#### Docking experiments (virtual screening) general procedure.

The MOE 2015.10 package was used to perform the docking studies between the refined TTR protein: A $\beta$  peptide system. Molecules computed as ligand for the docking experiments were pretreated using the LygX application from the software package MOE. After that the experiment were performed as follows: Alpha Triangle was used as placement method; Alpha HB as score function, and MMFF94x as forcefield in the first refinement step of the docking solutions. A rescoring step was also implemented in this computational pipeline, using London DG as function score, and again MMFF94x as forcefield for the last refinement step.

**Pharmacophore set-up.** The LigandScout 3.0 software package [65] was used to build-up a pharmacophore starting from the binding sites of TTR protein (T<sub>4</sub> binding pocket),  $\beta$ -secretase, metabotropic glutamate receptor 1 and metabotropic glutamate receptor 5. The pharmacophore resulting from this pocket alignment process was used to screen a set of molecules coming from the second pipeline explained in the next section.

**Selection pipeline of ligands.** Two complementary approaches were carried out to select the ligands to be docked in the TTR molecular model:

Pipeline A: starting from the Integrity database (<https://integrity.clarivate.com/integrity/xmlxsl/>), which contains small molecules and drugs in the market or advanced clinical phases, nearly 3200 compounds were selected and sorted according to which protein or disease was their main target: Amyloid peptide, transthyretin, both or Alzheimer's disease in general. In addition, nearly 500 compounds were also added to this list that have been gathered from the literature or that had been previously explored in our laboratories, as potential TTR stabilizers.

Then the CARLSBAD database and software [64], which contains integrated data on compounds and their target binding affinities, were used to select compounds that had experimentally shown affinity vs. both TTR and the amyloid peptide. This lead to a common stilbene substructure scaffold that was then used to carry out a substructure search among the original selection of nearly 3700 compounds. The resulting 48 compounds with the stilbene substructure were then docked into our TTR:A $\beta$  computational model [63].

Pipeline B: starting from the Integrity database (<https://integrity.clarivate.com/integrity/xmlxsl/>), which contains small molecules and drugs in the market or in advanced clinical phases, we selected nearly 1400 compounds that were reported in preclinical, clinical or marketed phase and that had their protein target reported as one or more of the following, which have been associated to AD: APP (amyloid precursor protein); AchE (acetylcholinesterase); IL-10 (interleukin-10);  $\alpha$ -,  $\beta$ - and  $\gamma$ -secretases; tau protein; GABA and glutamate receptors. All these compounds were then docked into the TTR model, prioritizing a pool of 134 molecules that would theoretically bind the TTR T<sub>4</sub> channel with an affinity similar to IDIF. These molecules were then virtually analyzed through docking with software MOE 2015.10 into the following protein structures: IL-10 (interleukin-10); inhibitor domain of APP (amyloid beta-protein precursor);  $\beta$ -secretase with inhibitor OM99-2; acetylcholinesterase (AChE) with Fasciculin-II; metabotropic glutamate receptor 1 with LY341495 antagonist; metabotropic glutamate receptor 5 with glutamate. All these docking processes lead to a prioritized list of 85 molecules, which were then docked into our TTR:A $\beta$  computational model [63], leading to 27 molecules that would theoretically bind to the TTR:A $\beta$  complex and to 4 additional AD related targets (A $\beta$ , IL-10,  $\beta$ -secretase and acetylcholinesterase). In addition, the initial set of

134 molecules that had been selected through docking with the TTR:A $\beta$  model, were further analyzed computationally through the software Ligand Scout; 13 of them coincided with the list of 27 molecules derived from the multi-target docking, but we were able to select 4 additional molecules that matched with the common pharmacophore.

The compounds prioritized through these two computational (*in silico*) complementary approaches that were commercially available (Molport, <http://www.molport.com>), were acquired, in order to carry out the experimental TTR binding, competition, and stability assays (See Table S1 in Supporting Information). Just only in few cases, if a selected compound was not commercially available but another compound with a very similar structure was available, then that similar compound was processed through the computational procedures described, and acquired if it would match with either the multi-target docking or the common pharmacophore filters. Finally, some compounds in the market and/or in clinical phases, that are reported in the literature as good TTR stabilizers and/or as AD therapies under clinical studies, were also analyzed through the computational filters described above, and included in the final list of compounds to be experimentally assayed.

**Recombinant wild-type human (wt rhTTR) production and purification.** Human wild type rhTTR gene was cloned into a pET expression system and transformed into *E. coli* BL21(DE3) Star [76]. The pHTRwt-1/pET-38b(+) plasmid was provided by Prof. Antoni Planas (IQS, URL) [77]. The production of recombinant protein was performed at Erlenmeyer scale, protein production and purification were done as described previously following an optimized version of our protocol [78]. wt rhTTR was produced using a pET expression System. The expressed protein only contains an additional methionine on the N-terminus if compared to the mature natural human protein sequence. wt rhTTR protein was expressed in *E. coli* BL21-(DE3) cells harboring the corresponding plasmid. Expression cultures in 2xYT rich medium containing 100  $\mu$ g/mL kanamycin were grown at 37 °C to an optical density (at 600 nm) of 4 (OD<sub>600</sub>  $\approx$  4), then induced by addition of IPTG (1 mM final concentration), grown at 37 °C for 20 h, and harvested by centrifugation at 4 °C, 10000 rpm for 10 min and resuspended in cell lysis buffer (0.5 M Tris-HCl, pH 7.6). Cell disruption and lysis were performed by French press followed by a sonication step at 4 °C. Cell debris were discarded after centrifugation at 4 °C, 11000 rpm for 30 min. Intracellular proteins were fractionated by ammonium sulfate precipitation in three steps. Each precipitation was followed by centrifugation at 12 °C, 12500 rpm for 30 min. The pellets were analyzed by SDS-PAGE (14% acrylamide). The TTR-containing fractions were resuspended in 20 mM Tris-HCl, 0.1 M NaCl, pH 7.6 (buffer A) and dialyzed against the same buffer. It was purified by ion exchange chromatography using a Q-Sepharose High Performance (Amersham Biosciences) anion exchange column and eluting with a NaCl linear gradient using 0.1 M NaCl in 20 mM Tris-HCl pH 7.6 buffer A to 0.5 M NaCl 20 mM Tris-HCl pH 7.6 (buffer B). All TTR-enriched fractions were dialyzed against deionized water in three steps and were lyophilized. The protein was further purified by gel filtration chromatography using a Superdex 75 prep grade resin (GE Healthcare BioSciences AB) and eluting with 20 mM Tris pH 7.6, 0.1 M NaCl. Purest fractions were combined and dialyzed against deionized water and lyophilized. The purity of protein preparations was >95% as judged by SDS-PAGE. Average production yields were 150–200 mg of purified protein per liter of culture. Protein concentration was determined spectrophotometrically at 280 nm using calculated extinction coefficient value of 17780 M<sup>-1</sup> cm<sup>-1</sup> for wtTTR. The protein was stored at -20 °C.

**Thyroxine binding assays.** Qualitative studies of the displacement of T<sub>4</sub> from WT TTR were carried out by incubation of 5  $\mu$ L of

human plasma, with  $^{125}\text{I}$ -T<sub>4</sub> (specific radioactivity  $\approx 1200 \mu\text{Ci}/\mu\text{g}$ ; PerkinElmer) in the presence of the different compounds (final concentration of  $666 \mu\text{M}$ ) [44,46]. Protein separation was carried out in a native PAGE system using glycine/acetate buffer. The gel was dried and revealed using an X-ray film.

For the quantitative analysis, T<sub>4</sub> binding competition assays based on a gel filtration procedure was used, as previously described [79]. Briefly, 50  $\mu\text{L}$  of a diluted sample (120 nM human recombinant TTR) was incubated with 50  $\mu\text{L}$  of either cold T<sub>4</sub> or compound solutions of variable concentrations ranging from 0 to 1000 nM and with a constant amount of labeled  $^{125}\text{I}$ -T<sub>4</sub> ( $\sim 50,000$  cpm). This solution was counted in a gamma spectrometer and incubated at 4 °C overnight. Protein bound  $^{125}\text{I}$ -T<sub>4</sub> and free  $^{125}\text{I}$ -T<sub>4</sub> were separated by gel filtration through a 1 ml BioGel P6DG (Bio-Rad) column. The bound fraction was eluted while free T<sub>4</sub> was retained on the BioGel matrix. The eluate containing the bound T<sub>4</sub> was collected and counted. Bound T<sub>4</sub> was expressed as percentage of total T<sub>4</sub> added. Each assay was performed in duplicate. Analysis of the binding data was performed with the GraphPad Prism program (version 5.0, San Diego, CA) and data was expressed as the EC50 ratio (EC50 T<sub>4</sub>/EC50 compound).

**TTR stability assay.** Recombinant wt-TTR (333  $\mu\text{M}$ ) was incubated alone or in the presence of different compounds for 1 h at 37 °C. Then, urea 8 M (used as denaturing agent) and sample buffer without SDS were added. Samples were then run in a 15% acrylamide gel, prepared without SDS, and transferred onto a nitrocellulose membrane (Amersham™ GE Healthcare – Protan 0.2  $\mu\text{m}$ ), using a wet system (Bio-Rad Criterion Blotter). The membranes were blocked 1 h at RT with 5% non-fat dry milk (DM) in PBS containing 0.05% Tween-20 (PBS-T) and then incubated with primary antibody anti-human TTR (Dako; 1:3000) in 3% DM/PBS-T. Then, washed membranes were incubated for 1 h at RT with sheep anti-rabbit immunoglobulins conjugated with horseradish peroxidase (The binding Site; 1:5000) in 3% DM/PBS-T. The blots were developed using Clarity™ Western ECL substrate (Bio-Rad) and levels of monomeric TTR were detected and visualized using a chemiluminescence detection system (ChemiDoc, Bio-Rad).

**Crystal structures of TTR:35 and TTR:73 complexes. Co-crystallization.** TTR (9.9 mg ml<sup>-1</sup>) was incubated with each compound (molar ratios 35/TTR = 20 and 73/TTR = 50) at 4 °C o.n., in HEPES buffer 10 mM, pH = 7.5. Crystals suitable for X-ray diffraction were obtained by hanging-drop vapour-diffusion techniques at 20 °C. Crystals were grown within 1 week by mixing 2  $\mu\text{L}$  of the protein:compound solutions with 2  $\mu\text{L}$  of reservoir solution. The reservoir solutions used in the crystallization trials contained acetate buffer 0.2 M pH 4.8–5.4, ammonium sulfate 1.8–2.2 M, 7% glycerol. Crystals were transferred to reservoir solutions containing increasing concentrations of glycerol (10–25%) and flash frozen in liquid nitrogen.

**Data collection, processing and refinement.** X-ray diffraction data sets were collected using synchrotron radiation at the XALOC beamline at the ALBA synchrotron center (Barcelona), ID30B beam line at the ESRF (European Synchrotron Radiation Facility, Grenoble Cedex, France) and Proxima 2 beam line at the SOLEIL synchrotron (Paris).

Diffraction images were processed with the XDS Program Package [80] and the diffraction intensities converted to structure factors in the CCP4 format [81]. A random 5% sample of the reflection data was flagged for R-free calculations [82] during model building and refinement. A summary of the data collection and refinement statistics is presented in Table S3. Initial molecular replacement phases were generated with PhaserMR [83], using as initial model one monomer of the complex TTR:IDIF (PDB ID 1Y1D) [52]. The final models were obtained after further cycles of refinement, carried out with Coot [84] and PHENIX [85].

**HTS ternary assay.** In this assay [28] the following stock solutions were used: Buffer A: 25 mM HEPES buffer, 10 mM glycine, pH 7.4 was prepared in the absence of salt. Protein (TTR) stock: 9.5 mg/mL (170  $\mu\text{M}$ ) in 25 mM HEPES buffer, 10 mM glycine, pH 7.4 and 5% DMSO (final concentration) was prepared in the absence of salt (buffer A). For the A $\beta$  peptide stock: 0.4 mg/mL (200  $\mu\text{M}$ ) in 25 mM HEPES buffer, 10 mM glycine, pH 7.4 and 5% DMSO (final concentration). For the small-molecule compound IDIF, a first solution of 3.76 mg/mL (10 mM) in DMSO was prepared. The final stock of the small-molecule IDIF was prepared by mixing 50  $\mu\text{L}$  of the previous DMSO solution with 950  $\mu\text{L}$  of buffer A (the final concentration of 5% DMSO).

First, the small-molecule compound and TTR complex was formed. To this end, 60  $\mu\text{L}$  of TTR stock was dispensed into the wells of a 96-well microplate. 40  $\mu\text{L}$  of small-molecule stock was added to give final concentrations of 100  $\mu\text{M}$ . The plate was introduced in the microplate reader (SpectraMax M5 Multi-Mode Microplate Readers, Molecular Devices Corporation, California, USA) and incubated for 1 h at 37 °C with orbital shaking 15 s every 30 min. Then, 100  $\mu\text{L}$  of A $\beta$  solution was added to the well to give a final concentration of 100  $\mu\text{M}$ .

Other wells of the 96-well microplate are filled with: a) Buffer alone: 200  $\mu\text{L}$  of buffer A solution was added to the well; b) Negative control of A $\beta$  aggregation: 200  $\mu\text{L}$  of A $\beta$ (1–11) stock solution in buffer A was dispensed into the wells; c) Testing TTR aggregation: 60  $\mu\text{L}$  of TTR stock were dispensed into the wells of a 96-well microplate and 140  $\mu\text{L}$  of buffer A were added; d) For the A $\beta$ (12–28) aggregation: 100  $\mu\text{L}$  of A $\beta$ (12–28) stock solution is dispensed into the wells and 100  $\mu\text{L}$  of buffer A were added; e) Testing if compounds interfere with A $\beta$ (12–28) aggregation.

The plate was incubated at 37 °C in a thermostated microplate reader with orbital shaking 15 s every minute for 30 min. The absorbance at 340 nm was monitored for 6 h at 30 min intervals. Data were collected and analyzed using Microsoft Excel software. All assays were done in duplicate.

$$RA (\%) = \left[ 1 - \left( \frac{Abs_c}{Abs_{A\beta} + Abs_c} \right) \right] * 100 \quad (1)$$

The parameter monitored in this assay was used to calculate the percent reduction of formation of aggregates (RA %) according to equation (1), where Abs<sub>A $\beta$</sub>  and Abs<sub>c</sub> are the final absorbance of the samples, in the absence or in the presence of the small-molecule compound/TTR complex; respectively.

**Thioflavin-T (ThT) fluorescence assays.** The robustness of our HTS turbidimetry-based method was further validated on the basis of comparative by Thioflavin-T (ThT) fluorescence assays on the same system. The ThT fluorescence was monitored at 37 °C using Gemini XPS plate reader (Molecular Devices) at an excitation wavelength of 440 nm and an emission wavelength of 490 nm. Thioflavin-T (ThT) was dissolved in 25 mM HEPES buffer, 10 mM glycine, pH 7.4 and 5% DMSO to a final concentration of 25  $\mu\text{M}$ . Aggregation of A $\beta$ (12–28) 50  $\mu\text{M}$  was performed in the presence of 25  $\mu\text{M}$  ThT. All solutions were dissolved in the same buffer. TTR was added to a final concentration of 25  $\mu\text{M}$ . IDIF was added to a final concentration of 50  $\mu\text{M}$ . Aggregation of A $\beta$ (1–42) 20  $\mu\text{M}$  was performed with 10  $\mu\text{M}$  TTR and 20  $\mu\text{M}$  of ligand. To test if selected compounds interfere with A $\beta$ (1–42) aggregation, aggregation of A $\beta$ (1–42) 20  $\mu\text{M}$  was performed with 20  $\mu\text{M}$  of ligands as an important control (Figs. S2–S11). For the ternary complex, TTR was incubated first with IDIF for 1 h, then A $\beta$ (12–28) was added. The final volume was 200  $\mu\text{L}$  for all samples. Fluorescence intensity at 490 nm of each sample was monitored after each 2 h for 8 h, and then at 21 h. Measurements were performed as independent triplicates. Recorded values were averaged and background

measurements (buffer containing 25  $\mu\text{M}$  ThT) were subtracted. Measurements were performed as independent triplicates. Recorded values were averaged and background measurements (buffer containing 25  $\mu\text{M}$  ThT) were subtracted.

**Isothermal Titration Calorimetry (ITC) studies.** Experiments were carried out in a VP-ITC (MicroCal, LLC, Northampton, Ma, USA). In a titration experiment [27], the ligand in the syringe is added in small aliquots to the macromolecule in our case TTR protein in the calorimeter cell, which is filled with an effective volume that is sensed calorimetrically. The TTR solution of 20  $\mu\text{M}$ , and A $\beta$  (A $\beta$ (12–28) or A $\beta$ (1–40)), or ligand solutions of 200  $\mu\text{M}$  were prepared in the same buffer. The titrant was injected over 20 or 30 times at a constant interval of 300 s with a 450 rpm rotating stirrer syringe into the sample cell containing its binding partner. All solutions were prepared with 25 mM HEPES buffer, 10 mM glycine, pH 7.4 and 5% DMSO (final concentration) and it was corroborated that at these conditions TTR and A $\beta$ (1–40) are stable. A $\beta$ (1–40) working solution was prepared at 200  $\mu\text{M}$  and used immediately, to avoid premature aggregate formation. TTR stock solution was prepared at 40  $\mu\text{M}$ . Ligand stock solution was prepared at 10 mM in DMSO. All solutions were prepared in the same buffer and filtered prior to use. In the control experiments, the titrant (ligand or A $\beta$ ) was injected into the buffer in the sample cell to measure the heat of dilution. This value of the heat of dilution was subtracted from the titration data. The experiments were performed at 25 °C. Titration data were analyzed by the evaluation software, MicroCal Origin, Version 7.0. The binding curves were fitted by a non-linear regression method to a one set of sites binding model. This leads to the calculation of  $K$ ,  $n$ ,  $\Delta H$ ,  $\Delta S$ , and  $\Delta G$ . Each experiment was conducted three times, and the mean value with standard deviations is provided.

#### Author contributions

The manuscript was written through contributions of all authors. All authors have given approval to the final version of the manuscript.

#### Funding sources

The work was supported by a grant from the Fundació Marató de TV3 (neurodegenerative diseases call, project reference: 20140330-31-32-33-34, <http://www.ccma.cat/tv3/marato/en/projectes-financats/2013/212/>). The group at IBMC-i3S also acknowledges for funding through grant Norte-01-0145-FEDER-000008 -Porto Neurosciences and Neurologic Disease Research Initiative at i3S, supported by Norte Portugal Regional Operational Programme (NORTE 2020), under the PORTUGAL 2020 Partnership Agreement, through the European Regional Development Fund (FEDER).

#### Notes

Dedicated to Dr. Gregorio Valencia.

#### Declaration of competing interest

The authors declare that they have no known competing financial interests or personal relationships that could have appeared to influence the work reported in this paper.

#### Acknowledgments

I. Cardoso works under the Investigator FCT Program which is financed by national funds through FCT and co-financed by ESF through HPOP, type 4.2 - Promotion of Scientific Employment. M.

Alemi was a recipient of a Research Fellowship (BIM) funded by the project of Fundació La Marató de TV3 (Spain), and L. M. Santos was a recipient of a fellowship from Norte 2020. J.P. Leite acknowledges the FCT fellowship SFRH/BD/129921/2017 (Portugal). IQAC-CSIC acknowledges a contract to Ellen Y. Cotrina funded by the project of Fundació Marató de TV3 (Spain) and a contract from Ford España - Fundación Apadrina la Ciencia (Spain). The group at CIC bioGUNE also acknowledges MINECO (Spain) for funding through grant CTQ2015-64597-C2-1-P and a Juan de la Cierva contract to A. Gimeno. We thank access to ALBA (XALOC), ESRF (ID30B) and Soleil (PROXIMA 1 and 2a) synchrotrons.

#### Appendix A. Supplementary data

Supplementary data to this article can be found online at <https://doi.org/10.1016/j.ejmech.2021.113847>.

#### Abbreviations

AChE	acetylcholinesterase
AD	Alzheimer Disease
APP	amyloid precursor protein
DMT	disease modifying therapy
CSF	cerebrospinal fluid
CP	choroid plexus
DIF	diflunisal
FAP	Familial Amyloid Polyneuropathy
FLU	flufenamic acid
GABA	gamma-aminobutyric acid
HTS	high throughput screening
IDIF	iododiflunisal
IPTG	Isopropyl $\beta$ -D-1-thiogalactopyranoside
LUT	luteolin
NSAID	non steroidal anti-inflammatory drug
OLS	olsalazine
o.n.	overnight
SDS-PAGE	sodium dodecyl sulfate polyacrylamide gel Electrophoresis
SMCs	small molecule chaperones
SUL	sulindac
TTR	transthyretin

#### References

- [1] Alzheimer's disease facts and figures, *Alzheimers Dement* (2020 Mar 10), <https://doi.org/10.1002/alz.12068>.
- [2] J. Cummings, N. Fox, Defining disease modifying therapy for alzheimer's disease, *J. Prev. Alzheimers Dis.* 4 (2017) 109–115, <https://doi.org/10.14283/jpad.2017.12>.
- [3] S. Dhillon, Aducanumab: first approval, *Drugs* (2021 Jul 29), <https://doi.org/10.1007/s40265-021-01569-z>.
- [4] R.E. Tanzi, FDA approval of Aduhelm paves a new path for alzheimer's disease, *ACS Chem. Neurosci.* 12 (2021) 2714–2715, <https://doi.org/10.1021/acscchemneuro.1c00394>.
- [5] G. Lalli, J.M. Schott, J. Hardy, B. De Strooper, Aducanumab: a new phase in therapeutic development for Alzheimer's disease? *EMBO Mol. Med.* (2021 Aug 2), e14781 <https://doi.org/10.15252/emmm.202114781>.
- [6] G.D. Rabinovici, Controversy and progress in alzheimer's disease - FDA approval of aducanumab, *N. Engl. J. Med.* (2021 Jul 28), <https://doi.org/10.1056/NEJMp2111320>.
- [7] J. Cummings, Drug development for psychotropic, cognitive-enhancing, and disease-modifying treatments for alzheimer's disease, *J. Neuropsychiatry Clin. Neurosci.* 33 (2021) 3–13.
- [8] J. Cummings, G. Lee, K. Zhong, J. Fonseca, K. Taghva, Alzheimer's disease drug development pipeline: 2021, *Alzheimers Dement (N Y)*. 7 (1) (2021 May 25), e12179, <https://doi.org/10.1002/trc2.12179>.
- [9] J. Cummings, Lessons learned from alzheimer disease: clinical trials with negative outcomes, *Clin. Transl. Sci.* 11 (2018) 147–152, <https://doi.org/10.1111/cts.12491>.
- [10] J.L. Molinuevo, C. Minguillon, L. Rami, J.D. Gispert, The rationale behind the new alzheimer's disease conceptualization: lessons learned during the last

- decades, *J. Alzheimers Dis.* 62 (2018) 1067–1077.
- [11] L.G. Friedman, N. McKeehan, Y. Hara, J.L. Cummings, D.C. Matthews, J. Zhu, R.C. Mohs, D. Wang, S.B. Hendrix, M. Quintana, L.S. Schneider, M. Grundman, S.P. Dickson, H.H. Feldman, J. Jaeger, E.C. Finger, J. Michael Ryan, D. Niehoff, S.L. Dickinson, J.T. Markowitz, M. Owen, A. Travaglia, H.M. Fillit, Value-generating exploratory trials in neurodegenerative dementias, *Neurology* (2021 Mar 5), <https://doi.org/10.1212/WNL.00000000000011774>.
- [12] J. Cummings, A. Ritter, K. Zhong, Clinical trials for disease-modifying therapies in alzheimer's disease: a primer, lessons learned, and a blueprint for the future, *J. Alzheimers Dis.* 64 (2018) S3–S22, <https://doi.org/10.3233/JAD-179901>.
- [13] C.C. Blake, M.J. Geisow, S.J. Oatley, B. Rerat, C. Rerat, Structure of prealbumin: secondary, tertiary and quaternary interactions determined by Fourier refinement at 1.8 Å, *J. Mol. Biol.* 121 (1978) 339–356.
- [14] T. Gião, J. Saavedra, E. Cotrina, J. Quintana, J. Llop, G. Arsequell, I. Cardoso, Undiscovered roles for transthyretin: from a transporter protein to a new therapeutic target for alzheimer's disease, *Int. J. Mol. Sci.* 21 (2020) 2075, <https://doi.org/10.3390/ijms21062075>.
- [15] A.L. Schwarzman, L. Gregori, M.P. Vitek, S. Lyubski, W.J. Strittmatter, J.J. Enghilde, R. Bhasin, J. Silverman, K.H. Weisgraber, P.K. Coyle, M.G. Zagorki, J. Talafous, M. Eisenberg, A.M. Saunders, A.D. Roses, D. Goldgaber, Transthyretin sequesters amyloid beta protein and prevents amyloid formation, *Proc. Nat. Acad. Sci. U. S. A.* 91 (1994) 8368–8372.
- [16] K.M. Pate, R.M. Murphy, Cerebrospinal fluid proteins as regulators of beta-amyloid aggregation and toxicity, *Isr. J. Chem.* 57 (2017) 602–612.
- [17] P. Davidsson, A. Westman-Brinkmalm, C.L. Nilsson, M. Lindbjör, L. Paulson, N. Andreasen, M. Sjögren, K. Blennow, Proteome analysis of cerebrospinal fluid proteins in Alzheimer patients, *Neuroreport* 13 (2002) 611–615.
- [18] J.M. Serot, D. Christmann, T. Dubost, M. Couturier, Cerebrospinal fluid transthyretin: aging and late onset Alzheimer's disease, *J. Neurol. Neurosurg. Psychiatry* 63 (1997) 506–550.
- [19] S.F. Gloeckner, F. Meyne, F. Wagner, U. Heinemann, A. Krasnianski, B. Meissner, I. Zerr, Quantitative analysis of transthyretin, tau and amyloid-beta in patients with dementia, *J. Alzheimers Dis.* 14 (2008) 17–25.
- [20] S.H. Han, E.S. Jung, J.H. Sohn, H.J. Hong, H.S. Hong, J.W. Kim, D.L. Na, M. Kim, H. Kim, H.J. Ha, Y.H. Kim, N. Huh, M.W. Jung, I. Mook-Jung, Human serum transthyretin levels correlate inversely with Alzheimer's disease, *J. Alzheimers Dis.* 25 (2011) 77–84, <https://doi.org/10.3233/JAD-2011-102145>.
- [21] L. Velayudhan, R. Killick, A. Hye, A. Kinsey, A. Güntert, S. Lynham, M. Ward, R. Leung, A. Lourdasamy, A.W. To, J. Powell, S. Lovestone, Plasma transthyretin as a candidate marker for Alzheimer's disease, *J. Alzheimers Dis.* 28 (2012) 369–375.
- [22] C.A. Ribeiro, I. Santana, C. Oliveira, I. Baldeiras, J. Moreira, M.J. Saraiva, I. Cardoso, Transthyretin decrease in plasma of MCI and AD patients: investigation of mechanisms for disease modulation, *Curr. Alzheimer Res.* 9 (2012) 881–889.
- [23] S.M. Oliveira, C.A. Ribeiro, I. Cardoso, M.J. Saraiva, Gender-dependent transthyretin modulation of brain amyloid- $\beta$  levels: evidence from a mouse model of Alzheimer's disease, *J. Alzheimers Dis.* 27 (2011) 429–439.
- [24] J.N. Buxbaum, Z. Ye, N. Reixach, L. Friske, C. Levy, P. Das, T. Golde, E. Masliah, A.R. Roberts, T. Bartfai, Transthyretin protects Alzheimer's mice from the behavioral and biochemical effects of A $\beta$  toxicity, *Proc. Natl. Acad. Sci. U.S.A.* 105 (2008) 2681–2686.
- [25] R. Costa, A. Gonçalves, M.J. Saraiva, I. Cardoso, Transthyretin binding to A-Beta peptide - impact on A-Beta fibrillogenesis and toxicity, *FEBS Lett.* 582 (2008) 936–942.
- [26] X. Li, X. Zhang, A.R.A. Ladiwala, D. Du, J.K. Yadav, P.M. Tessier, P.E. Wright, J.W. Kelly, J.N. Buxbaum, Mechanisms of transthyretin inhibition of  $\beta$ -amyloid aggregation in vitro, *J. Neurosci.* 33 (2013) 19423–19433.
- [27] E.Y. Cotrina, A. Gimeno, J. Llop, J. Jiménez-Barbero, J. Quintana, G. Valencia, I. Cardoso, R. Prohens, G. Arsequell, Calorimetric studies of binary and ternary molecular interactions between TTR, A $\beta$  peptides, and small-molecule chaperones toward an alternative strategy for AD drug discovery, *J. Med. Chem.* 63 (2020) 3205–3214.
- [28] E. Cotrina, A. Gimeno, J. Llop, J. Jiménez-Barbero, J. Quintana, R. Prohens, I. Cardoso, G. Arsequell, An assay for screening potential drug candidates for Alzheimer's disease that act as chaperones of the Transthyretin and Amyloid- $\beta$  peptides interaction, *Chemistry* 26 (2020) 17462–17469.
- [29] L. Nilsson, A. Pamrén, T. Islam, K. Brännström, S.A. Golchin, N. Pettersson, I. Iakovleva, L. Sandblad, A.L. Gharibyan, A. Olofsson, Transthyretin interferes with  $\beta$  amyloid formation by redirecting oligomeric nuclei into non-amyloid aggregates, *J. Mol. Biol.* 430 (2018) 2722–2733.
- [30] S.A. Ghadami, S. Chia, F.S. Ruggeri, G. Meisl, F. Bemporad, J. Habchi, R. Cascella, C.M. Dobson, M. Vendruscolo, T.P.J. Knowles, F. Chiti, Transthyretin inhibits primary and secondary nucleations of amyloid- $\beta$  peptide aggregation and reduces the toxicity of its oligomers, *Biomacromolecules* 21 (2020) 1112–1125.
- [31] M. Alemi, C. Gaiteiro, C.A. Ribeiro, L.M. Santos, J.R. Gomes, S.M. Oliveira, P.O. Couraud, B. Weksler, I. Romero, M.J. Saraiva, I. Cardoso, Transthyretin participates in beta-amyloid transport from the brain to the liver—involvement of the low-density lipoprotein receptor-related protein 1? *Sci. Rep.* 6 (2016 Feb 3) 20164.
- [32] J. Ricardo Vieira, A. Patrícia Moreira, Á. Oliveira, M. Alemi, I. Cardoso, Collagen type IV in brain vessels of an AD mouse model: modulation by transthyretin? *Amyloid* 26 (sup1) (2019) 138–139.
- [33] M.D. Howe, L.D. McCullough, A. Urayama, The role of basement membranes in cerebral amyloid angiopathy, *Front. Physiol.* 11 (2020 Nov 25) 601320, <https://doi.org/10.3389/fphys.2020.601320>.
- [34] P. Kerschen, V. Planté-Bordeneuve, Current and future treatment approaches in transthyretin familial amyloid polyneuropathy, *Curr. Treat. Options Neurol.* 18 (12) (2016) 53.
- [35] D. Adams, C. Cauquil, C. Labeyrie, Familial amyloid polyneuropathy, *Curr. Opin. Neurol.* 30 (2017) 481–489.
- [36] I. Cardoso, C.S. Goldsburly, S.A. Müller, V. Olivieri, S. Wirtz, A.M. Damas, U. Aebi, M.J. Saraiva, Transthyretin fibrillogenesis entails the assembly of monomers: a molecular model for in vitro assembled transthyretin amyloid-like fibrils, *J. Mol. Biol.* 317 (2002) 683–695.
- [37] M.R. Almeida, L. Gales, A.M. Damas, I. Cardoso, M.J. Saraiva, Small transthyretin (TTR) ligands as possible therapeutic agents in TTR amyloidosis, *Curr. Drug Targets - CNS Neurol. Disord.* 4 (2005) 587–596.
- [38] D. Adams, C. Cauquil, C. Labeyrie, G. Beaudonnet, V. Algalarrondo, M. Théaudin, TTR kinetic stabilizers and TTR gene silencing: a new era in therapy for familial amyloidotic polyneuropathies, *Expert Opin. Pharmacother.* 17 (2016) 791–802.
- [39] S.M. Johnson, R.L. Wiseman, Y. Sekijima, N.S. Green, S.L. Adamski-Werner, J.W. Kelly, Native state kinetic stabilization as a strategy to ameliorate protein misfolding diseases: a focus on the transthyretin amyloidosis, *Acc. Chem. Res.* 38 (2005) 911–921.
- [40] T. Yokoyama, M. Mizuguchi, Transthyretin amyloidogenesis inhibitors: from discovery to current developments, *J. Med. Chem.* 3 (2020) 14228–14242.
- [41] S. Nencetti, E. Orlandini, TTR fibril formation inhibitors: is there a SAR? *Curr. Med. Chem.* 19 (2012) 2356–2379.
- [42] G. Ortore, A. Martinelli, Identification of novel transthyretin fibril formation inhibitors using structure-based virtual screening, *ChemMedChem* 12 (2017) 1327–1334.
- [43] C.J. Simões, T. Mukherjee, R.M. Brito, R.M. Jackson, Toward the discovery of functional transthyretin amyloid inhibitors: application of virtual screening methods, *J. Chem. Inf. Model.* 50 (2010) 1806–1820.
- [44] S. Connelly, D.E. Mortenson, S. Choi, I.A. Wilson, E.T. Powers, J.W. Kelly, S.M. Johnson, Semi-quantitative models for identifying potent and selective transthyretin amyloidogenesis inhibitors, *Bioorg. Med. Chem. Lett* 27 (2017) 3441–3449.
- [45] S.K. Palaninathan, Nearly 200 X-Ray crystal structures of transthyretin: what do they tell us about this protein and the design of drugs for TTR amyloidosis? *Curr. Med. Chem.* 19 (2012) 2324–2342.
- [46] T. Coelho, G. Merlini, C.E. Bulawa, J.A. Fleming, D.P. Judge, J.W. Kelly, M.S. Maurer, V. Planté-Bordeneuve, R. Labaudinière, R. Mundayat, S. Riley, I. Lombardo, P. Huertas, Mechanism of action and clinical application of Tafamidis in hereditary transthyretin amyloidosis, *Neurol. Ther.* 5 (2016) 1–25.
- [47] S. Nencetti, A. Rossello, E. Orlandini, Tafamidis (Vyndaqel): a light for FAP patients, *ChemMedChem* 8 (2013) 1617–1619.
- [48] R. Sant'Anna, P. Gallego, L.Z. Robinson, A. Pereira-Henriques, N. Ferreira, F. Pinheiro, S. Esperante, I. Pallares, O. Huertas, M.R. Almeida, N. Reixach, R. Insa, A. Velazquez-Campoy, D. Reverter, N. Reig, S. Ventura, Repositioning tolcapon as a potent inhibitor of transthyretin amyloidogenesis and associated cellular toxicity, *Nat. Commun.* 7 (2016 Feb 23) 10787.
- [49] C.A. Ribeiro, M.J. Saraiva, I. Cardoso, Stability of the transthyretin molecule as a key factor in the interaction with A-beta peptide – relevance in Alzheimer's disease, *PLoS One* 7 (9) (2012), e45368, <https://doi.org/10.1371/journal.pone.0045368>.
- [50] M.R. Almeida, B. Macedo, I. Cardoso, I. Alves, G. Valencia, G. Arsequell, A. Planas, M.J. Saraiva, Selective binding to transthyretin and tetramer stabilization in serum from patients with familial amyloidotic polyneuropathy by an iodinated diflunisal derivative, *Biochem. J.* 381 (2004) 351–356.
- [51] T. Mairal, J. Nieto, M. Pinto, M.R. Almeida, L. Gales, A. Ballesteros, J. Barluenga, J.J. Pérez, J.T. Vázquez, N.B. Centeno, M.J. Saraiva, A.M. Damas, A. Planas, G. Arsequell, G. Valencia, Iodine atoms: a new molecular feature for the design of potent transthyretin fibrillogenesis inhibitors, *PLoS One* 4 (2009) e4124, <https://doi.org/10.1371/journal.pone.0004124>.
- [52] L. Gales, S. Macedo-Ribeiro, G. Arsequell, G. Valencia, M.J. Saraiva, A.M. Damas, Human transthyretin in complex with iododiflunisal: structural features associated with a potent amyloid inhibitor, *Biochem. J.* 388 (2005) 615–662.
- [53] C.A. Ribeiro, S.M. Oliveira, L.F. Guido, A. Magalhaes, G. Valencia, G. Arsequell, M.J. Saraiva, I. Cardoso, Transthyretin stabilization by iododiflunisal promotes amyloid- $\beta$  peptide clearance, decreases its deposition, and ameliorates cognitive deficits in an Alzheimer's disease mouse model, *J. Alzheimers Dis.* 39 (2014) 357–370, <https://doi.org/10.3233/JAD-131355>.
- [54] L. Rejc, V. Gómez-Vallejo, X. Rios, U. Cossio, Z. Baz, e. Mujica, T. Gião, E.Y. Cotrina, J. Jiménez-Barbero, J. Quintana, G. Arsequell, I. Cardoso, J. Llop, Oral treatment with iododiflunisal delays beta amyloid plaque formation in a transgenic mouse model of Alzheimer Disease: a Longitudinal in vivo molecular imaging study, *J. Alzheimer's Dis.* 2020 (Pub Date : 2020-08-10) (2020) <https://doi.org/10.21203/rs.2.23011/v1>.
- [55] A. Martorana, U. Perricone, A. Lauria, The repurposing of old drugs or unsuccessful lead compounds by in silico approaches: new advances and perspectives, *Curr. Top. Med. Chem.* 16 (2016) 2088–2106.
- [56] T.I. Oprea, J.P. Overington, Computational and practical aspects of drug repositioning, *Assay Drug Dev. Technol.* 13 (2015) 299–306.
- [57] V. Parvathaneni, N.S. Kulkarni, A. Muth, V. Gupta, Drug repurposing: a

- promising tool to accelerate the drug discovery process, *Drug Discov. Today* 24 (2019) 2076–2085.
- [58] A. Corbett, G. Williams, C. Ballard, Drug repositioning in Alzheimer's disease, *Front. Biosci. (Schol Ed)* 7 (2015) 184–188.
- [59] T.W. Kim, Drug repositioning approaches for the discovery of new therapeutics for Alzheimer's disease, *Neurotherapeutics* 12 (2015) 132–142.
- [60] S. Rodriguez, C. Hug, P. Todorov, N. Moret, S.A. Boswell, K. Evans, G. Zhou, N.T. Johnson, B.T. Hyman, P.K. Sorger, M.W. Albers, A. Sokolov, Machine learning identifies candidates for drug repurposing in Alzheimer's disease, *Nat. Commun.* 12 (1) (2021 Feb 15) 1033, <https://doi.org/10.1038/s41467-021-21330-0>.
- [61] A. Anighoro, J. Bajorath, G. Rastelli, Polypharmacology: challenges and opportunities in drug discovery, *J. Med. Chem.* 57 (2014) 7874–7887.
- [62] L. Calzà, V.A. Baldassarro, A. Giuliani, L. Lorenzini, M. Fernandez, C. Mangano, S. Sivilia, M. Alessandri, M. Gusciglio, R. Torricella, L. Giardino, From the multifactorial nature of Alzheimer's disease to multitarget therapy: the contribution of the translational approach, *Curr. Top. Med. Chem.* 13 (2012) 1843–1852.
- [63] A. Gimeno, L.M. Santos, M. Alemi, J. Rivas, D. Blasi, Y. Cotrina, J. Llop, G. Valencia, I. Cardoso, J. Quintana, G. Arsequell, J. Jiménez-Barbero, Insights on the interaction between transthyretin and A $\beta$  in solution. A saturation transfer difference (std) NMR analysis of the role of iododiflunisal, *J. Med. Chem.* 60 (2017) 5749–5758.
- [64] S.L. Mathias, J. Hines-Kay, J.J. Yang, G. Zahoransky-Kohalmi, C.G. Bologna, O. Ursu, T.I. Oprea, The CARLSBAD database: a confederated database of chemical bioactivities. Database (Oxford). 2013 Jun 21, bat044, <http://datascience.unm.edu/carlsbad-platform/carlsbad/>, 2013.
- [65] G. Wolber, T. Langer, LigandScout: 3-D pharmacophores derived from protein-bound ligands and their use as virtual screening filters, *J. Chem. Inf. Model.* 45 (2005) 160–169.
- [66] L.M. Santos, D. Rodrigues, M. Alemi, S.C. Silva, C.A. Ribeiro, I. Cardoso, Resveratrol administration increases Transthyretin protein levels ameliorating AD features- importance of transthyretin tetrameric stability, *Mol. Med.* 22 (2016) 597–607.
- [67] W.M. Partridge, Treatment of alzheimer's disease and blood-brain barrier drug delivery, *Pharmaceuticals* 13 (11) (2020) 394, <https://doi.org/10.3390/ph13110394>.
- [68] X. Rios, V. Gómez-Vallejo, A. Martín, U. Cossío, M.Á. Morcillo, M. Alemi, I. Cardoso, J. Quintana, J. Jiménez-Barbero, E.Y. Cotrina, G. Valencia, G. Arsequell, J. Llop, Radiochemical examination of transthyretin (TTR) brain penetration assisted by iododiflunisal, a TTR tetramer stabilizer and a new candidate drug for AD, *Sci. Rep.* 9 (1) (2019 Sep 20) 13672, <https://doi.org/10.1038/s41598-019-50071-w>.
- [69] J.P. Modi, H. Prentice, J.Y. Wu, Sulindac for stroke treatment: neuroprotective mechanism and therapy, *Neural Regen Res* 9 (2014) 2023–2025.
- [70] D. Sawmiller, S. Li, M. Shahaduzzaman, A.J. Smith, D. Obregon, B. Giunta, C.V. Borlongan, P.R. Sanberg, J. Tan, Luteolin reduces Alzheimer's disease pathologies induced by traumatic brain injury, *Int. J. Mol. Sci.* 15 (2014) 895–904.
- [71] M.A. Ajmone-Cat, A. Bernardo, A. Greco, L. Minghetti, Non-steroidal anti-inflammatory drugs and brain inflammation: effects on microglial functions, *Pharmaceuticals* 3 (2010) 1949–1965.
- [72] W.M. Partridge, Blood-brain barrier delivery, *Drug Discov. Today* 12 (1–2) (2007) 54–61.
- [73] D.E. Clark, In silico prediction of blood-brain barrier permeation, *Drug Discov. Today* 8 (2003) 927–933.
- [74] Molecular Operating Environment (MOE), Chemical computing group ULC, Montreal, QC, Canada, H3A 2R7, in: 1010 Sherbooke St. West, Suite #910, 2013.08, 2017. URL, <http://chemcomp.com/>.
- [75] D.A. Case, T.A. Darden, T.E. Cheatham, C.L. Simmerling, J. Wang, R.E. Duke, R. Luo, M. Crowley, R.C. Walker, W. Zhang, K.M. Merz, B. Wang, S. Hayik, A. Roitberg, G. Seabra, I. Kolossvary, K.F. Wong, F. Paesani, J. Vanicek, X. Wu, S.R. Brozell, T. Steinbrecher, H. Gohlke, L. Yang, C. Tan, J. Mongan, V. Hornak, G. Cui, D.H. Mathews, M.G. Seetin, C. Sagui, V. Babin, P.A. Kollman, *AMBER 10* (2008) [Google Scholar].
- [76] H. Furuya, M.J. Saraiva, M.A. Gawinowicz, I.L. Alves, P.P. Costa, H. Sasaki, I. Goto, Y. Sakaki, Production of recombinant human transthyretin with biological activities toward the understanding of the molecular basis of familial amyloidotic polyneuropathy (FAP), *Biochemistry* 30 (1991) 2415–2421.
- [77] I. Dolado, J. Nieto, M.J.M. Saraiva, G. Arsequell, G. Valencia, A. Planas, Kinetic assay for high-throughput screening of in vitro transthyretin amyloid fibrillogenesis inhibitors, *J. Comb. Chem.* 7 (2005) 246–252.
- [78] E.Y. Cotrina, M. Vilà, J. Nieto, G. Arsequell, A. Planas, Preparative scale production of recombinant human transthyretin for biophysical studies of protein-ligand and protein-protein interactions, *Int. J. Mol. Sci.* 21 (24) (2020) 9640.
- [79] M.R. Almeida, I.L. Alves, H. Terazaki, Y. Ando, M.J. Saraiva, Comparative studies of two transthyretin Variants with protective effects on familial amyloidotic polyneuropathy: TTR R104H and TTR T119M, *Biochem. Biophys. Res. Commun.* 270 (2000) 1024–1028.
- [80] W. Kabsch, Automatic processing of rotation diffraction data from crystals of initially unknown symmetry and cell constants, *J. Appl. Crystallogr.* 26 (1993) 795–800.
- [81] Collaborative Computational Project, Number 4, The CCP4 suite: programs for protein crystallography, *Acta Crystallogr. D Biol. Crystallogr.* 50 (1994) 760–763.
- [82] A.T. Brünger, Free R value: a novel statistical quantity for assessing the accuracy of crystal structures, *Nature* 355 (1992) 472–475.
- [83] A.J. McCoy, R.W. Grosse-Kunstleve, P.D. Adams, M.D. Winn, L.C. Storoni, R.J. Read, Phaser crystallographic software, *J. Appl. Crystallogr.* 40 (2007) 658–674.
- [84] P. Emsley, B. Lohkamp, W.G. Scott, K. Cowtan, Features and development of Coot, *Acta Crystallogr. D Biol. Crystallogr.* 66 (2010) 486–501.
- [85] P.D. Adams, P.V. Afonine, G. Bunkóczi, V.B. Chen, I.W. Davis, N. Echols, J.J. Headd, L.W. Hung, G.J. Kapral, R.W. Grosse-Kunstleve, A.J. McCoy, N.W. Moriarty, R. Oeffner, R.J. Read, D.C. Richardson, J.S. Richardson, T.C. Terwilliger, P.H. Zwart, PHENIX: a comprehensive Python-based system for macromolecular structure solution, *Acta Crystallogr. D Biol. Crystallogr.* 66 (2010) 213–221.